ELSEVIER

Journal of Nuclear Materials 313–316 (2003) 1081–1084

journal of nuclear materials

www.elsevier.com/locate/jnucmat

The influence of the divertor magnetic configuration and of ELM frequency on target heat fluxes in MAST

A. Kirk [a,*], J.-W. Ahn [b], G.F. Counsell [a], The MAST Team

[a] *EURATOM/UKAEA Fusion Association, D3 Culham Science Centre, Abingdon, Oxon, Oxfordshore OX14 3DB, UK*
[b] *Imperial College of Science, Technology and Medicine, University of London, London SW7 2BZ, UK*

Abstract

ELM characteristics in a large spherical tokamak with significant auxiliary heating are explored. Access to H-mode is significantly easier when the plasma magnetic configuration is near to a connected double null. The change in ELM frequency with core density and/or auxiliary heating power is broadly similar to conventional devices of a similar size in the type III regime. Power at the targets during an ELM arrives predominantly at the outboard side, irrespective of ELM frequency. The data are consistent with transport into the scrape-off layer being driven predominantly by diffusive processes in quiescent periods between ELMs, and thus being distributed roughly according to the 4:1 ratio of outboard to inboard separatrix surface areas. In L-mode and during ELMs themselves, however, the transport is augmented by turbulent processes, which are more prominent at the outboard side, where the field is very low and where the magnetic surfaces have bad curvature.

PACS: 52.40.Hf
Keywords: ELMs; Magnetic configuration; H-mode access; Divertor power load

1. Introduction

Divertor power handling in the spherical tokamak (ST) is of even greater significance than in conventional devices due to the reduced area of the inboard strike-points. A good understanding of the effects of ELMs on target power loading is central to evaluating the potential of the ST as a future burning device.

MAST is well equipped with edge plasma diagnostics. Of particular note are the arrays of high spatial and temporal resolution Langmuir probes covering all four targets (3 mm spacing inboard, 10 mm spacing outboard). The fast sweep (65 μs) on each individual probe allows data to be resolved in periods much shorter than an ELM duration (typically a few hundred μs). The probes have been operated in two modes: (1) one strike-point is covered and each probe is read out once per 65 μs; and (2) in a multiplexed mode where all strike-points are covered but each probe is read out once per 1 ms. In the former method a series of 'identical' shots were required in order to explore all four strike-points. In the latter case a data 'box-car' technique has been used to obtain target profiles both at ELM peaks and inter-ELM, during regular ELMing periods. In this method the target profiles are built up at each strike-point by requiring that the probe information was collected within 30 μs of the desired time point (either ELM peak or inter-ELM time). The results from each method are found to be consistent.

The power density arriving at each of the target probes was calculated from the ion saturation current density (J_{SAT}) and the electron temperature (T_e) using $P = \gamma J_{SAT} T_e$, taking the sheath transmission coefficient $\gamma = 7$ [1]. Exponential fits to the spatial power profile in both the scrape-off layer (SOL) and private flux region

* Corresponding author. Tel.: +44-1235 466846; fax: +44-1235 466379.
E-mail address: andrew.kirk@ukaea.org.uk (A. Kirk).

0022-3115/03/$ - see front matter
PII: S0022-3115(02)01541-6

are then used to calculate the total power flowing to each target by integrating over the strike-point regions. Data collected from the probe arrays over a large number of shots have been used to explore the characteristics and operating regimes of the MAST SOLs in L-mode and ELMy H-mode plasmas.

2. Effect of magnetic configuration

The most common operating mode for MAST is the disconnected double-null (DDN) in which the two X-points lie on different flux surfaces with the gap between these at the mid-plane, $\partial_{r_{sep}}$, being of the order of the ion gyro-radius. Fig. 1(a) shows a plot of the ratio of total integrated power arriving at the outboard strike-point to the inboard strike-point (P_{oi}) as a function of $\partial_{r_{sep}}$ for a series of shots with a constant P_{SOL} (defined as the sum of the Ohmic and auxiliary power input to the core plasma less the change in stored energy and radiated power). Firstly, it can be seen that H-mode access is achieved for small $\partial_{r_{sep}}$ i.e. when the plasma is near to a connected double null (CDN) configuration. Secondly, in the L-mode cases the ratio P_{oi} is dependent on $\partial_{r_{sep}}$ which determines the degree of isolation between the inboard and outboard SOLs. A similar effect was observed on DIII-D [2]. For small separation the ratio P_{oi} is 30 and since $P_{outer} + P_{inner} \approx P_{SOL}$ this implies that 96% of the power leaving the core flows into the outboard SOL. This is much larger than would be expected from the ratio of the surface area of the separatrices (≈4) and would suggest that the outboard power efflux is augmented by other processes, perhaps turbulence related to the bad curvature and very low field on the outboard mid-plane. Finally, the P_{oi} ratio at the ELMs is compatible with the L-mode ratio for a similar $\partial_{r_{sep}}$; however, the inter-ELM ratio is much smaller. Fig. 1(b) shows a histogram of how the ratio P_{oi} changes as a function of ELM frequency, using from more than 100 analysed ELMy H-mode discharges. Each point represents the weighted mean of the data in that bin and the error bar represents the standard deviation of the distribution. Firstly, independent of ELM frequency most of the power in the ELMs flows to the outboard strike-point, with the ratio highest at higher ELM frequencies when more than 95% of the power reaches the outboard side. Secondly, in the inter-ELM period the ratio P_{oi} tends to the ratio of the outboard to inboard separatrix surface area (≈4) at low ELM frequency. Thus the additional processes, which increased the relative power flow to the outboard side in L-mode and at the ELMs, are absent or strongly suppressed.

3. Effect of ELM frequency

Fig. 2(a) and (b) show the ELM frequency as a function of line-averaged density and P_{SOL} respectively. The decrease of ELM frequency with decreasing density and increasing power is typical of type III ELMs [3].

Fig. 3 shows a plot of the ratio of the integrated power arriving at the ELM to inter-ELM as a function of ELM frequency for the outboard and inboard strike-points. Firstly, independent of frequency the ratio is ≈1 for the inboard strike-points consistent with very little of the power released by the ELMs reaching the inboard targets. For the outboard targets the ratio rises with decreasing ELM frequency reaching an average ratio of greater than 5 for ELMs below 250 Hz. The maximum peak power densities observed to date during an ELM,

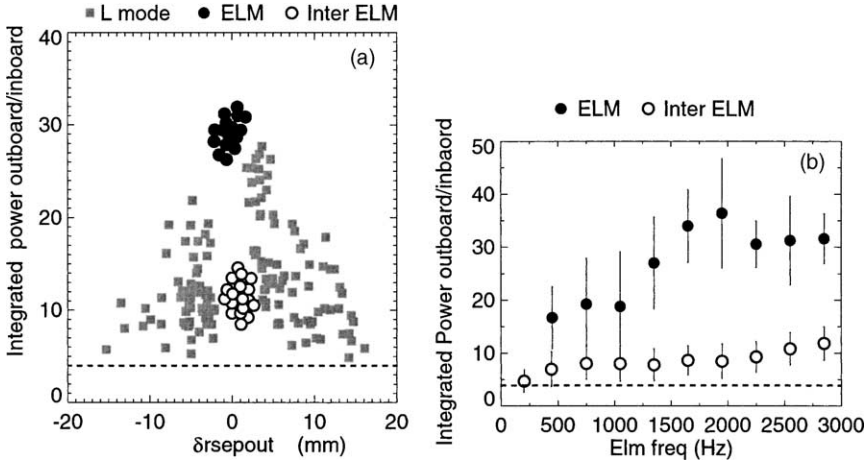

Fig. 1. The ratio of the integrated power to outboard over inboard targets: (a) versus $\delta_{r_{sep}}$ for L-mode and H-mode discharges at constant P_{SOL} and (b) versus ELM frequency for ELM and inter-ELM periods during H-mode discharges at constant $\delta_{r_{sep}}$. The dashed line shows the ratio of outboard to inboard separatrix areas.

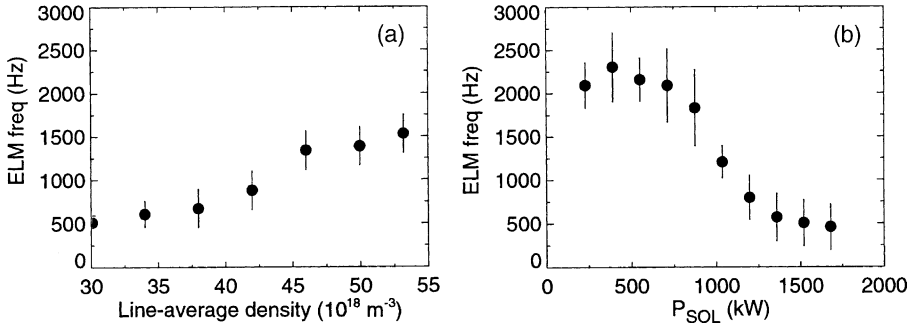

Fig. 2. ELM frequency versus line-average density for $P_{SOL} > 1$ MW and ELM frequency versus P_{SOL} for line-average density in the range (30–40) $\times 10^{18}$ m^{-3}.

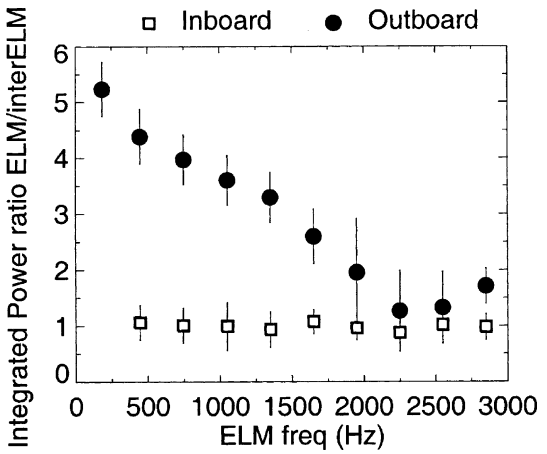

Fig. 3. Ratio of the integrated power at the ELM to the inter-ELM for the inboard and outboard strike-points as a function of ELM frequency.

for P_{SOL} up to 2 MW, are 2 MW m^{-2} at the inboard strike-points and 4 MW m^{-2} at the outboard strike-points.

The rise in peak power density at the ELM is due mainly to an increase in the J_{SAT}. The electron temperature at the outboard side rises by a factor of 1.5 at the ELM relative to inter-ELM and the rise is effectively independent of ELM frequency. The arrival of the ELM at the outboard target is accompanied by an outward shift in radius of the peak power position by up to 2 cm for low frequency ELMs. The H-mode strike-point widths are 20% narrower than the L-mode widths. However, there is no significant change in the width of the distribution from inter-ELM to ELM.

4. Integrating over the ELM peak and inter-ELM period

Emission of D_α light in the divertor region has been used to determine the duration of the ELM peak (≈300 μs) and the inter-ELM period. During these two periods the probe power and density measurements have been integrated over time to produce the energy and the number of particles arriving at the probes respectively. As the ELM frequency decreases and hence the inter-ELM period increases, and recalling that very little power from the ELM reaches the inboard side, the energy deposited at the inboard targets is greater during the inter-ELM period than at the ELM, reaching a maximum value of 40 J. For the outboard targets the ratio of energy deposited during an ELM to the inter-ELM period is ≈1 independent of frequency. The energy deposited increases with decreasing ELM frequency reaching a maximum value of 600 J at low ELM frequencies.

The number of particles in the plasma can be estimated by multiplying the line averaged plasma density determined from the CO_2 interferometer by the plasma volume calculated by EFIT [4]. A drop in the line-averaged density is observed at each ELM and this drop can be used to estimate the fraction of particles released during an ELM. Fig. 4(a) shows the fraction of particles emitted at an ELM calculated using the line-averaged density and from the number of particles arriving at the probes during an ELM. For $\bar{n}_e > 3.5 \times 10^{19}$ m^{-3}, where the MAST SOL is observed to be in a high-recycling regime [5], the number of particles observed at the probes is greater than the number of particles emitted from the core, as would be expected from flux amplification [1]. However, in the sheath limited regime $\bar{n}_e < 3.5 \times 10^{19}$ m^{-3}, good agreement is found between the number of particles emitted from the core and those arriving at the targets. At low ELM frequencies, up to 3% of the particles in the core are emitted during an ELM. These results are similar to those observed in Compass-D [6].

The energy emitted during the ELM has been calculated from the change in stored energy from EFIT, using EFIT runs with a 200 μs time step. The fraction of energy stored in the plasma emitted at an ELM is shown in Fig. 4(b) together with the figure calculated from the

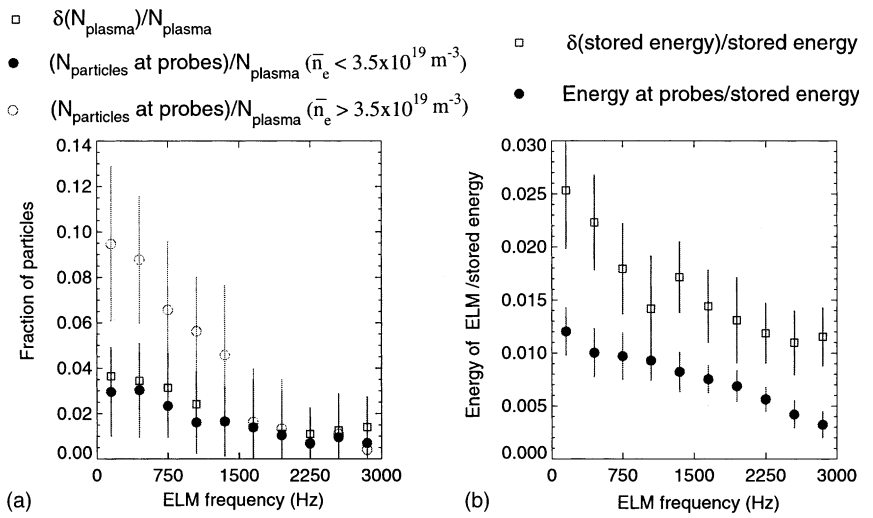

Fig. 4. (a) The fraction of particles in the plasma emitted in an ELM measured by the target probes and from the change of the plasma density. For the target probes the number of particles arriving during the same time interval during an inter-ELM period have been subtracted giving the excess number of particles associated with an ELM. (b) The fraction of stored plasma energy released by an ELM measured by the target probes and from the change of stored energy from EFIT.

energy arriving at the probes. The fraction calculated from EFIT is approximately a factor of 2 greater than the value from the probes. Since the bolometry does not indicate a significant increase in radiated power, a possible explanation is that a large fraction of the ELM energy flows in the ion channel i.e. T_i was substantially greater than T_e.

5. Summary and conclusions

The ELM properties of a large ST have been characterised in some detail for the first time, using the extensive edge diagnostics available on the MAST device. MAST typically operates in a slightly asymmetric DDN configuration, which is found to aid H-mode access. The power loading at the targets in MAST has been characterised for L-mode and ELMy H-mode plasmas at plasma currents up to 1 MA and with up to 2 MW of neutral beam heating. The change in ELM frequency with core density and/or auxiliary heating power is broadly similar to conventional devices of a similar size in the type III regime. Power flow to the divertor targets has been evaluated from target Langmuir probe data. In L-mode, the total power arriving at all four targets accounts for nearly 100% of P_{SOL} and is distributed mostly towards the outboard targets, the outboard to inboard ratio of power effluxes being typically $P_{oi} \sim 30$ for near CDN discharges. In ELMy H-mode, the ratio remains around $P_{oi} \sim 30$ at the ELM peak for high ELM frequencies but falls to a minimum of around $P_{oi} \sim 4$ during long inter-ELM periods, at lower ELM frequency. At the ELM peaks themselves, P_{oi} remains around 20 indicating that up to 95% of energy released from the core during ELMs flows to the outboard SOL. The data are consistent with transport into the SOL being driven predominantly by diffusive processes in quiescent periods between ELMs, and thus being distributed roughly according to the 4:1 ratio of outboard to inboard separatrix surface areas. In L-mode and actually during ELMs, however, the transport is augmented by turbulent processes that are more prominent at the outboard side, where the field is very low and where the magnetic surfaces have bad curvature. At low ELM frequencies, up to 3% of the particles in the core are released during an ELM, which is comparable to the change of plasma density.

Acknowledgements

This work is jointly funded by Euratom and the UK Department of Trade and Industry. Dr Ahn would like to recognise the support of a grant from the British Foreign and Commonwealth office.

References

[1] P.C. Stangeby, Physics of Plasma–Wall Interactions in Controlled Fusion, Plenum, 1986.
[2] E.J. Doyle et al., Phys. Fluids B 3 (1991) 2300.
[3] T.W. Petrie et al., J. Nucl. Mater. 290–293 (2001) 931.
[4] L.L. Lao et al., Nucl. Fusion 25 (1985) 1611.
[5] G.F. Counsell et al., Plasma Phys. Control. Fusion 44 (2002) 1.
[6] M. Valovic et al., Proceedings of the 23rd EPS Conference on Controlled Fusion and Plasma Physics, 20 C, 1996, p. 39.